Functional properties and differential mode of regulation of the nitrate transporter from a plant symbiotic ascomycete

Barbara MONTANINI*[1], Arturo R. VISCOMI*, Angelo BOLCHI*, Yusé MARTIN†, José M. SIVERIO†, Raffaella BALESTRINI‡, Paola BONFANTE‡ and Simone OTTONELLO*[2]

*Dipartimento di Biochimica e Biologia Molecolare, Università di Parma, 43100 Parma, Italy, †Instituto Universitario de Enfermedades Tropicales y Salud Pública, Departamento de Bioquímica y Biología Molecular, Grupo del Metabolismo del Nitrógeno, Universidad de La Laguna, E-38206, La Laguna, Spain, and ‡Dipartimento di Biologia Vegetale, Università di Torino and Istituto per la Protezione delle Piante (Sezione di Micologia), Consiglio Nazionale delle Ricerche, 10125 Torino, Italy

Nitrogen assimilation by plant symbiotic fungi plays a central role in the mutualistic interaction established by these organisms, as well as in nitrogen flux in a variety of soils. In the present study, we report on the functional properties, structural organization and distinctive mode of regulation of TbNrt2 (*Tuber borchii* NRT2 family transporter), the nitrate transporter of the mycorrhizal ascomycete *T. borchii*. As revealed by experiments conducted in a nitrate-uptake-defective mutant of the yeast *Hansenula polymorpha*, TbNrt2 is a high-affinity transporter ($K_m = 4.7\ \mu$M nitrate) that is bispecific for nitrate and nitrite. It is expressed in free-living mycelia and in mycorrhizae, where it preferentially accumulates in the plasma membrane of root-contacting hyphae. The TbNrt2 mRNA, which is transcribed from a single-copy gene clustered with the nitrate reductase gene in the *T. borchii* genome, was specifically up-regulated following transfer of mycelia to nitrate- (or nitrite)-containing medium. However, at variance with the strict nitrate-dependent induction commonly observed in other organisms, TbNrt2 was also up-regulated (at both the mRNA and the protein level) following transfer to a nitrogen-free medium. This unusual mode of regulation differs from that of the adjacent nitrate reductase gene, which was expressed at basal levels under nitrogen deprivation conditions and required nitrate for induction. The functional and expression properties, described in the present study, delineate TbNrt2 as a versatile transporter that may be especially suited to cope with the fluctuating (and often low) mineral nitrogen concentrations found in most natural, especially forest, soils.

Key words: gene regulation, *Hansenula polymorpha*, mycorrhiza, nitrate/nitrite transport, nitrogen deficiency, *Tuber borchii* NRT2 family transporter (TbNrt2).

INTRODUCTION

Nitrate is a major source of nitrogen for a variety of organisms, including mycorrhizal fungi and their plant hosts, and it is often the nutrient that limits their growth. On a global scale, reduced nitrogen derived from nitrate assimilation is estimated to exceed, by approx. two orders of magnitude, the amount of nitrogen that is assimilated via nitrogen fixation. Prior to reductive assimilation through the action of NR (nitrate reductase) and NIR (nitrite reductase), nitrate is internalized via an energy-dependent uptake process by specific plasma membrane transporters. A large group of NTs (nitrate transporters), from both prokaryotes and eukaryotes, belong to the MFS (major facilitator superfamily) and, specifically, to the *NRT2* family of NT-encoding genes [1–3]. The most well characterized fungal members of this family are NrtA (formerly known as CrnA) and NrtB from *Aspergillus nidulans* [4–6] and Ynt1 from *Hansenula polymorpha* [7,8]. They share a similar membrane topology, in which two sets of six TM (transmembrane) helices, with an $N_{IN}C_{IN}$ (N-terminus intracellular/C-terminus intracellular) orientation, are connected by a large cytosolic loop. Two NT genes have been identified in *A. nidulans* [6], whereas only one is present in *Ha. polymorpha* [3] and *Neurospora crassa* (*nit-10*; [9]). Fungal NT genes, with some exceptions (e.g. *nit-10*), are usually clustered with NR and NIR genes and are generally induced by nitrate and repressed by reduced nitrogen sources such as ammonium and glutamine [3,4,9,10].

Particularly interesting, although so far very little explored, are nitrate transporters from plant symbiotic fungi, such as the ectomycorrhizal ascomycete *Tuber borchii* addressed in the present study. In these organisms, which colonize most tree species in temperate forests, soil-retrieved nitrogen not only serves for self-nutrition, but also is a key player in the mutualistic nitrogen/carbon trade established with the plant host. This bidirectional nutrient exchange takes place in specialized symbiotic structures, called ectomycorrhizae, which connect the extraradical fungal mycelium to the root system, thereby dramatically expanding the effective surface area for nutrient soil exploration. Investigations carried out over the last few decades have provided ample evidence as to the contribution of ectomycorrhizae to plant nitrogen status and have highlighted their crucial ecological role in nitrogen cycling within forest ecosystems ([11,12] and references therein). This renewed perception of the ecological importance of ectomycorrhizae has revived efforts to elucidate the molecular processes underlying nitrogen assimilation and the related starvation stress responses in ectomycorrhizal fungi [13–15]. A number of genes coding for

Abbreviations used: EST, expressed sequence tag; GST, glutathione S-transferase; MFS, major facilitator superfamily; NCBI, National Center for Biotechnology Information; $N_{IN/OUT}$, N-terminus intracellular/extracellular; NIR, nitrite reductase; NR, nitrate reductase; NS, nitrate signature; NT, nitrate transporter; ORF, open reading frame; SSM, synthetic solid medium; TbNrt2, *Tuber borchii* NRT2 family transporter; TM, transmembrane.

[1] Present address: UMR INRA/UHP 1136, Interactions Arbres/Micro-organismes, Université Henri Poincaré-Nancy I, 54506 Vandoeuvre-les-Nancy, France.

[2] To whom correspondence should be addressed (email s.ottonello@unipr.it).

The nucleotide sequences reported in this paper have been submitted to the GenBank®, DDBJ and EMBL databases under the accession numbers AF462038 (TbNrt2 coding region) and AY786418 (TbNrt2 upstream non-coding region).

ammonium transporters and nitrogen assimilation enzymes have been isolated from these organisms [16–22]. In contrast, only one gene coding for an as yet functionally uncharacterized NT has been identified so far in a mycorrhizal fungus, the basidiomycete *Hebeloma cylindrosporum* [23]. At variance with the requirement for both nitrogen catabolite derepression and nitrate-mediated induction commonly displayed by nitrate assimilation components, the mRNA for this NT was found to be up-regulated by nitrogen deprivation in the absence of nitrate. Such a mode of regulation, which is shared by the NR and NIR genes of *He. cylindrosporum* [16,23], has thus far been documented only in this organism. This raises a question as to whether it represents a unique feature of this species or an adaptive trait of plant symbiotic fungi in general, and whether additional molecular features may distinguish the NTs (and other nitrate assimilation components) of symbiotic fungi from their saprotrophic counterparts.

In the present study, we report the functional, structural and expression analysis of TbNrt2 (*T. borchii* NRT2 family transporter), the NT of *T. borchii*, a plant symbiotic ascomycete that grows in a nitrification-proficient soil habitat, is reportedly beneficial to its host plants and is closely related evolutionarily to the fungi whose NTs have been the most well characterized so far. TbNrt2 is a plasma-membrane-localized high-affinity NT that is bispecific for nitrate and nitrite, and expressed in free living mycelia as well as in root-contacting hyphae. It responds positively to nitrate supplementation, but also to nitrogen starvation alone, thus pointing to nitrate-independent up-regulation as a functional signature of NTs from symbiotic fungi. Interestingly, however, TbNrt2 regulation differs from that of the adjacent NR gene, which was found to be up-regulated in a strictly nitrate-dependent manner, as in most nitrate utilizing organisms. The possible ecophysiological significance of this differential mode of regulation is discussed.

EXPERIMENTAL

Biological materials

T. borchii Vittad. mycelia (isolate ATCC 95640) were grown in the dark at 23 °C on a SSM (synthetic solid medium), either complete or deprived of a single nutrient, as described previously [18]. Single nitrogen sources were utilized for all shift experiments, except those involving nitrate, which was also supplied in combination with NH_4Cl, glutamine or proline.

Isolation of the *TbNrt2* cDNA

A cDNA library constructed in the excisable phage vector Uni-Zap XR from 20-day-old *T. borchii* mycelia (a gift from Dr A. Viotti, Istituto di Biologia e Biotecnologia Agraria, CNR, Milano, Italy) was used as a source of template DNA (100 ng/reaction) for PCR amplifications. The oligonucleotides 5′-GCCCTGCGCTTCTTCATCGG-3′ (plus) and 5′-AAATGGCCGGCATGACGAAG-3′ (minus), designed on a highly conserved region of fungal and plant NTs characterized previously [1], were used for the amplification of the *TbNrt2* cDNA. Amplification reactions were conducted under the following 'touch-down' PCR conditions: 2 min of initial denaturation at 94 °C, 20 cycles of 30 s denaturation at 94 °C and 30 s annealing at progressively lower temperatures (from 60 to 51 °C) with a decrease of 1 °C every other cycle, followed by 30 additional cycles at an annealing temperature of 50 °C. The DNA fragment obtained from such amplification was cloned into the pGEM-T-easy vector (Promega), sequence-verified, and used as a probe for plaque-hybridization analysis of the *T. borchii* cDNA library [24]. A cDNA of 1770 bp (*TbNrt2*) was thus identified, excised to produce plasmid pBlueScript-SK-*TbNrt2*, sequenced on both strands and compared with known NT genes using BLASTX. Standard PCR conditions were used to map the upstream located *tbnr1* gene (GenBank® accession number AF533362). The *tbnr1–TbNrt2* intergenic sequence was amplified by PCR using 50 ng of genomic DNA as the template and the 5′-GACGAGTGATCCATGATGATG-3′ (plus)/5′-ATAAGAGACTCAACTGCATGTG-3′ (minus) oligonucleotides as primers. The resulting amplicon (1660 bp) was cloned into the SmaI site of pBlueScript-SK (Stratagene) and sequenced on both strands. The *tbnr1–TbNrt2* intergenic sequence (see Figure 1C) was assembled manually by overlapping the above 1644 bp sequence (between positions −1641 and +3 of *TbNrt2*; numbered with respect to the ATG start site) with part of the 5′-UTR (untranslated region) of *tbnr1* (positions −2187/−1453, with respect to the *TbNrt2* ATG).

Functional assays in the yeast *Ha. polymorpha*

A 1523-bp-long fragment containing the *TbNrt2* ORF (open reading frame; 1503 bp in length) plus 13 bp and 7 bp of 5′- and 3′-flanking DNA respectively, was cloned into the SalI and SpeI sites of the pYNR-EX vector, bearing the promoter and terminator elements of the *Ha. polymorpha* NR (*YNR1*) gene [25], to generate pYNR-EX-*TbNrt2*. The wild-type strain NCYC495 of *Ha. polymorpha* and its derivative strains harbouring a disrupted version of either the NT gene (Δ*ynt1::URA3 LEU2*) or the NR gene (Δ*ynr1::URA3*), or both (Δ*ynt1::URA3* Δ*ynr1::URA3*) [3,7] were used in the present study. Yeasts were grown with orbital shaking in liquid YG medium [0.17 % yeast nitrogen base without amino acids and ammonium sulphate (Difco), supplemented with 2 % (w/v) glucose] plus the indicated nitrogen sources. Yeast transformation was carried out as described previously [26] with 1 μg of pYNR-EX-*TbNrt2* DNA, linearized with BstII to target integration into the *LEU2* locus [25]. The Δ*ynt1* status of recipient cells and their transformation by pYNR-EX-*TbNrt2* were verified by PCR analysis using the following sets of primers: 5′-CGGAATTCACATGTGATAGTGTT-3′ (plus)/5′-GCACATGTAGCAAAGTCC-3′ (minus) for the *YNT1* locus; and 5′-GCAGCAATGATACAT-3′ (plus)/5′-TATCCAACTTGCGCG-3′ (minus) for the *YNR1* locus.

Nitrate transport was measured by determining the rate of extracellular nitrate depletion as described previously [8]. Similar experimental conditions, except for the replacement of $NaNO_3$ with $NaNO_2$ and the use of a 25 mM Mes/Tris (pH 6.0) medium, were used for nitrite-uptake assays. Chlorate sensitivity was determined by serial dilution growth tests conducted in parallel on wild-type, Δ*ynt1* disruptant and *YNT1*-disrupted pYNR-EX-*TbNrt2*-transformed (Δ*ynt1TbNrt2*) strains. Cells were spotted on to YG agar containing 5 mM $NaNO_3$ and 1 mM proline, plus increasing concentrations of $KClO_3$ (from 50 up to 200 mM); plates were incubated at 37 °C and photographed after 3 days.

DNA and RNA analyses

Genomic DNA samples for gel-blot analysis (4 μg each) were digested with BamHI, EcoRI and HindIII, and electrophoresed on 0.8 % agarose gels. A random priming labelling kit (Amersham Biosciences) was used for ^{32}P-labelling of *TbNrt2* hybridization probes. Blotting on to Hybond-N (Amersham Biosciences), pre-hybridization and high-stringency washing were conducted according to the manufacturer's instructions. Total RNA for RNase protection and RNA gel-blot assays was isolated and quantified as described previously [13]. A ^{32}P-labelled antisense riboprobe (332 nt) was prepared by *in vitro* T7 RNA polymerase transcription of FokI-digested pBlueScript-SK-*TbNrt2*.

Saturating amounts of a *T. borchii* β-tubulin riboprobe (259 nt) were added to all reactions as an internal standard. Hybridization (5 μg of total RNA/assay), RNase A/T1 digestion and gel fractionation were carried out as described previously [13]. Protected fragments were visualized by autoradiography and quantified with a Personal Imager FX using the Multi-Analyst/PC software (Bio-Rad Laboratories). Heat-denatured total RNA (20 μg for each sample) fractionated on glyoxal-agarose gels, transferred on to a nylon membrane and hybridized with a ^{32}P-labelled full-length *TbNrt2* cDNA probe was used for high-stringency RNA gel-blot analysis [24]. Blotting on to GeneScreen Plus (PerkinElmer Life Science), pre-hybridization and washing were conducted according to the manufacturer's instructions. The same radioactive labelling and hybridization procedures were applied to *tbnr1*; a 405-bp DNA fragment (positions 1125–1529) prepared by PCR was used as a probe. Superscript III reverse transcriptase (Invitrogen) and total RNA (5 μg) from mycelia that had been nitrogen-starved for 7 days were used for primer extension analysis [24]. Template RNA and a radioactively labelled primer (5′-ATAGGAAGGCAATCATGAATCCGAATGTGC-3′), encompassing positions 112–142 of the *TbNrt2* coding region, were heat-denatured (7 min at 80 °C) and annealed at 42 °C for 1 h. After addition of the enzyme and other reaction components, reverse transcription was allowed to proceed for 1 h at 50 °C. Extended cDNA fragments were ethanol-precipitated, electrophoretically fractionated on a denaturing sequencing gel and compared with the products of a sequencing reaction carried out with *TbNrt2* DNA using the same primer as above.

DNA and protein sequence analysis

Six different programs, set to standard parameters and relying on single sequence predictions, were used to analyse the membrane topology of TbNrt2. These are available at the following addresses: MEMSAT2 (http://bioinf.cs.ucl.ac.uk/psipred/; [31]); TopPred2 (http://bioweb.pasteur.fr/seqanal/interfaces/toppred.html; [34]); HMMTOP (http://www.enzim.hu/hmmtop/html/adv_submit.html; [36]); TMHMM2 (http://www.cbs.dtu.dk/services/TMHMM/; [35]); TMpred (http://www.ch.embnet.org/software/TMPRED_form.html; [32]); TMAP (http://www.mbb.ki.se/tmap/; [33]). The SSpro8 program (http://www.igb.uci.edu/tools/scratch/; [38]) was used to predict β-turn regions. Sequence similarity searches were conducted with BLAST on the non-redundant (nr) protein database at the NCBI (National Center for Biotechnology Information; http://www.ncbi.nlm.nih.gov/). The fungal genome databases at MIT (Massachusetts Institute of Technology; http://www.broad.mit.edu/index.html), MIPS (Munich Information Center for Protein Sequences; http://mips.gsf.de/) and JGI (Department of Energy Joint Genome Institute; http://www.jgi.doe.gov/sequencing/), and the EST (expressed sequence tag) database at the NCBI plus the EST collection at COGEME (Consortium for the Functional Genomics of Microbial Eukaryotes; http://www.cogeme.man.ac.uk/) were used to search for TbNrt2 homologues. Predicted polypeptide sequences were aligned with CLUSTAL W [27]. Phylogenetic analysis was conducted with the neighbour-joining algorithm implemented in CLUSTAL X [27a]. Phylogenetic trees were visualized with TreeView [28]. The programs 'motif search' (http://www.genome.ad.jp/), relying on the TRANSFAC database, and NNPP/Eukaryotic (eukaryotic promoter prediction by neural network) and TESS (search for transcription factor binding sites), at the BCM (Baylor College of Medicine) Search Launcher server (http://searchlauncher.bcm.tmc.edu/), were used to search for putative control elements in the 5′-flanking region of *TbNrt2*.

Immunoblot and immunofluorescence analyses

A polypeptide corresponding to the VI–VII loop region of TbNrt2 (amino acid positions 219–314; see Figure 4A) fused to bacterial GST (glutathione S-transferase) within the pGEX-4T-2 expression vector (Amersham Biosciences) was used as antigen for anti-TbNrt2 antibody production. Standard procedures were used for recombinant protein expression and purification (GSTrap application note, Amersham Biosciences) and rabbit immunization. Crude membrane fractions for immunoblot analysis were prepared from both *Ha. polymorpha* and *T. borchii* as described previously [8]. Balanced amounts of the various fractions, containing the same amount of total protein quantified with the Coomassie Brilliant Blue G-250 dye (Pierce Biotechnology, Inc.) method, were first fractionated on 12 % (w/v) polyacrylamide gels [8], transferred to Hybond-ECL® (Amersham Biosciences) and analysed with horseradish-peroxidase-conjugated anti-(rabbit IgG) antibodies and enhanced chemiluminescence reagents (Pierce Biotechnology) according to the manufacturer's instructions. Parallel reactions carried out on untransformed *Ha. polymorpha* cells or with the use of the pre-immune serum were used as specificity controls. Immunofluorescence analysis was conducted on *in-vitro*-produced *T. borchii*/*Cistus incanus* mycorrhizae [29]. Root segments were fixed overnight at 4 °C with 4 % (v/v) paraformaldehyde in PBS (pH 7.4). After washing with PBS, they were embedded in 8 % (w/v) low-melting agarose. Sections (100 μm thick), prepared with a Balzer Vibratome series 1.000 apparatus, were incubated overnight at 4 °C with the anti-TbNrt2 serum (diluted 1:500–1:1000) in 50 mM phosphate buffer (pH 7.2) containing 1 % (w/v) BSA. Sections were washed three times (15 min each) with 50 mM phosphate buffer (pH 7.2), saturated for 30 min with 1 % (w/v) BSA in 50 mM phosphate buffer, and incubated at room temperature in the dark for 3 h with FITC-conjugated goat anti-(rabbit IgG) (diluted 1:80). Sections were then washed as before, mounted and analysed with a Leica TCS SP2 confocal microscope, using the 488 nm Ar laser band to excite both FITC fluorescence and paraformaldehyde-induced tissue autofluorescence. The two signals were discriminated with wavelength-specific emission filters: 500–540 nm for FITC (false-coloured in green) and 590–630 nm for tissue autofluorescence (false-coloured in red). Labelling specificity was assessed by replacing the primary antibody with either buffer alone or buffer with pre-immune serum.

RESULTS

Isolation and sequence analysis of TbNrt2

Oligonucleotide primers designed on a conserved region of known NTs from fungi, plants and the alga *Chlamydomonas reinhardtii* were initially employed for PCR amplification experiments conducted on a *T. borchii* mycelium cDNA library. A 159-bp-long DNA fragment matching the sequences of the above NTs was obtained and used as a probe for library screening. Five hybridization-positive cDNAs were identified, the longest of which, named *TbNrt2* (1770 bp; GenBank® accession number AF462038), was sequenced and found to contain a 1503-nt-long ORF, starting with an initiator ATG and lying in a good sequence context according to translation initiation rules in fungi [30]. The predicted translation product of the *TbNrt2* cDNA is 501 amino acids in length with an estimated molecular mass of 54.2 kDa. A single mRNA of approx. 1800 nt was revealed by a high-stringency RNA gel-blot analysis using the full-length *TbNrt2* cDNA as a probe. An essentially single-band pattern, shown in Figure 1(A), was also obtained when *T. borchii* genomic DNA, digested with either HindIII, BamHI or EcoRI, was hybridized

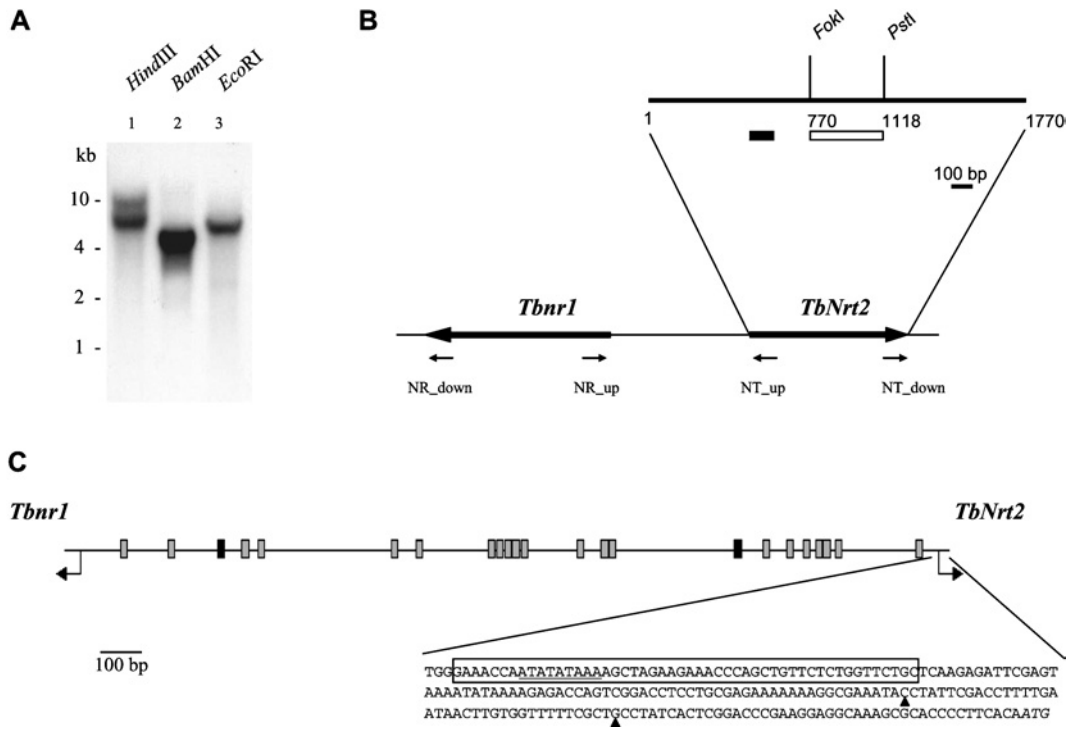

Figure 1 DNA gel blot and 5′-flanking region analysis of *TbNrt2*

(**A**) *T. borchii* genomic DNA digested with HindIII (lane 1), BamHI (lane 2) or EcoRI (lane 3) was probed with a ^{32}P-labelled *TbNrt2*-derived DNA fragment (shown in **B**). The migration positions of DNA size markers run alongside are indicated on the left. (**B**) Restriction map of the *TbNrt2* cDNA and localization of the adjacent NR (*tbnr1*) gene. The positions of the DNA probe (black bar) and of the antisense riboprobe (white bar) used for DNA gel-blot and RNase-protection analyses respectively, as well as the annealing positions of the four oligonucleotide primers used for *tbnr1* localization and the head-to-head orientation of *TbNrt2* and *tbnr1*, are indicated. Arrows indicate the position and orientation of the two primer pairs utilized to amplify the intergenic region interposed between *tbnr1* and *TbNrt2*. (**C**) Sequence analysis of the *TbNrt2–tbnr1* intergenic region (2187 bp). Nit2- and Nit4-like control elements are represented as grey and black boxes respectively. The sequence of the 200-bp region upstream of the *TbNrt2* initiator ATG (shown in italic) is reported. The two main transcription start sites identified by primer extension analysis (arrowheads at positions −44 and −81), as well as the putative promoter region (boxed) and the TATA-box (underlined), are indicated.

with a cDNA probe (159 bp) not containing recognition sites for any of the above restriction enzymes. The fainter hybridizing band observed in the HindIII digestion mixture did not change appreciably when the same blot was hybridized under low-stringency conditions (results not shown). While not excluding the possible existence of NT paralogues, as in *A. nidulans* [6], the data indicate that *TbNrt2* is a single-copy gene in the *T. borchii* genome. Also shown (Figure 1B) are the results of PCR amplification experiments using mixed primer pairs derived from *TbNrt2* and from the NR gene of *T. borchii* (*tbnr1*; [20]). Only one of the four mixed primer pairs used for these experiments (made up by an upstream annealing, *TbNrt2*-derived oligonucleotide and by an oligonucleotide complementary to the most upstream part of *tbnr1*) led to successful amplification, with the production of an approx. 1700-bp-long amplicon. Thus, even though no information on the genomic localization of the NIR gene is currently available, it appears that at least two nitrate assimilation genes are clustered in the genome of *T. borchii*. Further support for the NT identity of *TbNrt2* was provided by sequence analysis of its 5′-flanking region (GenBank® accession number AY786418), which was found to contain a number of putative control elements resembling the binding sites of nitrogen status-dependent regulators in other filamentous fungi, especially the Nit2 and Nit4 regulators of *N. crassa* [9,10] (Figure 1C).

Functional properties of the TbNrt2 transporter

The nitrate transport ability of TbNrt2 was tested by functional complementation assays carried out in an NT-disrupted strain of the yeast *Ha. polymorpha* (Δ*ynt1*), which is unable to grow on media containing 0.5 mM nitrate as the sole nitrogen source and to transport nitrate at concentrations lower than 0.5 mM [7]. The Δ*ynt1* strain was transformed with the integrative expression vector pYNR-EX-*TbNrt2* in which the *TbNrt2* ORF is under the control of the promoter and terminator elements of the *Ha. polymorpha* NR (*YNR1*) gene [25]. Six transformants capable of growing on 0.5 mM $NaNO_3$ were randomly picked and their *YNT1*-disrupted status, as well as their integrative transformation with pYNR-EX-*TbNrt2*, was verified and validated by PCR analysis (results not shown). One such transformant (named *YM5*) was chosen for further analysis. The expression of TbNrt2 in the Δ*ynt1* strain bearing the chimaeric pYNR-EX-*TbNrt2* construct was determined by immunoblotting using an antiserum raised against the VI–VII loop of TbNrt2 (amino acids 219–314; see Figure 4A). As revealed by the immunoblot in Figure 2(A), a major polypeptide of 54 kDa along with a minor band of approx. 40 kDa (most probably a degradation product of the larger polypeptide) were recognized by the anti-TbNrt2 serum in crude membrane preparations derived from the Δ*ynt1TbNrt2* transformant, but not from the untransformed isogenic strain. The molecular mass of the larger immunopositive polypeptide is the same as that predicted for TbNrt2, thus indicating that the pYNR-EX-*TbNrt2* construct supports the synthesis of the putative *T. borchii* NT in *Ha. polymorpha* cells. Importantly, the same *TbNrt2* transformant is capable of growing in the presence of a nitrate concentration (0.5 mM) that is not sufficient for growth of *Δynt1* cells (Figure 2B). As shown in Figure 3(A), the YM5 strain is capable of taking up nitrate, albeit with an efficiency that

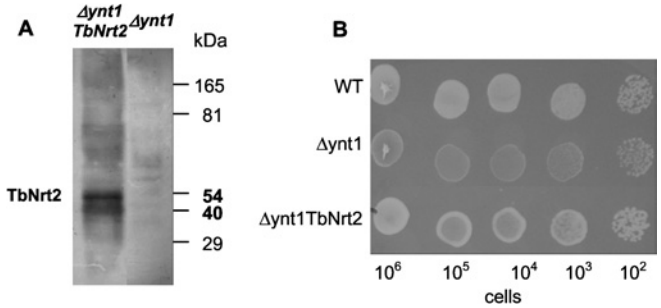

Figure 2 Functional and expression analysis of TbNrt2 in *Ha. polymorpha*

(**A**) Immunoblot analysis of TbNrt2 in crude membrane preparations (10 μg of total protein) derived from the pYNR-EX-*TbNrt2* transformed strain (Δ*ynt1-TbNrt2*) and from the *YNT1*-disrupted untransformed isogenic strain (Δ*ynt1*). The estimated molecular masses of the polypeptides recognized by the anti-TbNrt2 serum (54 and 40 kDa) and the migration positions of molecular-mass markers (in kDa) are indicated on the right. (**B**) Rescue of yeast growth in the presence of a limiting nitrate concentration. Serial dilutions of wild-type (WT), Δ*ynt1* and Δ*ynt1TbNrt2* cells were spotted on to YG agar containing 500 μM $NaNO_3$ as the sole nitrogen source and incubated for 3 days at 37 °C.

is approx. 3-fold lower than that of wild-type cells. This reduced transport rate may be due to the use of a heterologous promoter, to a sub-optimal plasma membrane targeting and/or impaired stability in the heterologous host, or to an intrinsically lower transport capacity (and/or affinity for nitrate ions) of TbNrt2 compared with Ynt1. To distinguish between the latter two possibilities, we determined the apparent kinetic parameters for nitrate transport by TbNrt2. As shown in Figure 3(B), nitrate transport by the Δ*ynt1TbNrt2* transformant was saturable, with apparent K_m and V_{max} values (derived from Lineweaver–Burk and Eadie-Hoffstee analyses of the data) of 4.7 ± 0.8 μM and 0.18 ± 0.01 nmol $\cdot$ min^{-1} $\cdot$ mg^{-1} of cells respectively. Although the V_{max} was difficult to compare with values reported previously because of uncertainties concerning expression levels and plasma membrane localization, the K_m value, which was independent of the number of active TbNrt2 molecules, appeared to be close to those reported previously for *Ha. polymorpha* Ynt1 [8] and for the high-affinity NrtB transporter from *A. nidulans* [6]. Therefore sub-optimal accumulation and/or membrane targeting, rather than an intrinsically reduced affinity for nitrate ions, are likely to be responsible for the lower nitrate uptake activity of TbNrt2 in *Ha. polymorpha*.

The nitrite transport capacity of TbNrt2 was examined next. In *Ha. polymorpha*, it has been shown that, at pH 6.0, nearly all nitrite transport takes place through Ynt1 in such a way that, in a Δ*ynt1* strain, the transport of this ion was negligible compared with that of the wild-type strain [8]. As revealed by the results of nitrite transport assays conducted in the Δ*ynt1* mutant and in the corresponding *TbNrt2* transformant (Figure 3C), TbNrt2 restored nitrite transport capacity. Although the kinetic parameters were not determined, the data indicate that the K_m for nitrite transport was also in the micromolar range. What was also apparent, however, was that the rate of nitrite uptake at 50 μM $NaNO_2$ was lower than that measured at 12.5 μM. Based on previous results in *Ha. polymorpha* [8], this behaviour probably reflects the cellular toxicity of nitrite, due to a concentration-dependent nitrite-induced uncoupling effect. Additional proof of the nitrite transport capacity of TbNrt2 was obtained from experiments (results not shown) that showed the ability of nitrate to competitively inhibit such a process. The ability of TbNrt2 to take up chlorate, thus leading to cell poisoning, was also examined. As revealed by serial dilution growth tests carried out at increasing chlorate concentrations (50–200 mM), the

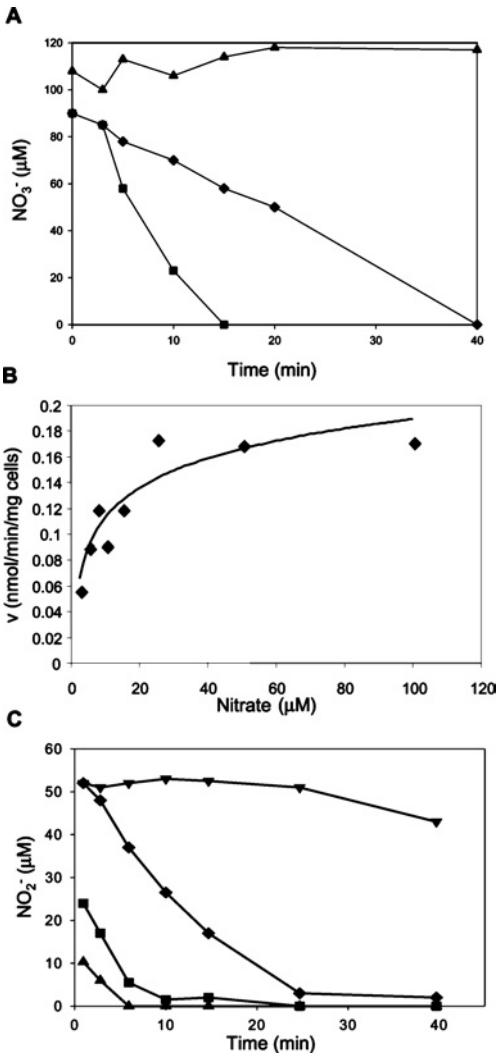

Figure 3 Nitrate and nitrite transport by TbNrt2

(**A**) Time-course of nitrate uptake. Transport assays were started with the addition of 100 μM $NaNO_3$ to cells previously exposed to nitrate and were conducted for the indicated times on Δ*ynt1* (▲), *WT* (■) and Δ*ynt1TbNrt2* (◆) strains. (**B**) Concentration-dependence of nitrate uptake by Δ*ynt1TbNrt2* cells. The rate of nitrate uptake (v) by a *TbNrt2* transformant (YM5) was assayed as in (**A**) at the indicated nitrate concentrations. (**C**) Nitrite uptake by TbNrt2. Transport assays, started with the addition of $NaNO_2$ to cells previously exposed to nitrate, were conducted for the indicated lengths of time on a Δ*ynt1TbNrt2* transformant grown in YG medium (pH 6.0) containing 50 μM (◆), 25 μM (■) or 12.5 μM (▲) $NaNO_2$; untransformed Δ*ynt1* control cells (▼) were assayed in parallel in the presence of 50 μM $NaNO_2$.

Δ*ynt1TbNrt2* transformant grew as well as Δ*ynt1* and wild-type cells in the presence of chlorate concentrations up to 100 mM, whereas all strains were incapable of growing in the presence of 200 mM chlorate (results not shown). Although not ruling out the possibility that TbNrt2 may transport chlorate (albeit with an exceedingly high K_m), the data clearly point to its unappreciable contribution to chlorate toxicity in *Ha. polymorpha*.

Membrane topology and phylogenetic relationships of TbNrt2

Six different prediction programs (MEMSAT2, TMpred, TMAP, TopPred2, TMHMM2 and HMMTOP) were used to construct a model of TbNrt2, reliably predicting the localization and orientation of individual TM helices. Five of these programs predicted 12 TM helices with an $N_{IN}C_{IN}$ topology, whereas one less TM helix and an $N_{OUT}C_{IN}$ (N-terminus extracellular/C-terminus

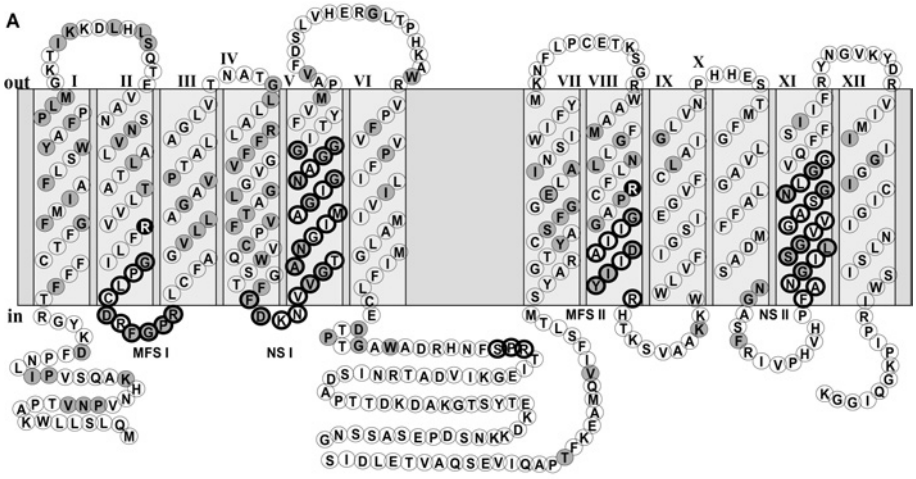

	I	II	III	IV	V	VI	VII	VIII	IX	X	XI	XII
TopPred	**34**-54	74-94	**100**-120	130-**150**	161-181	**198-218**	315-**335**	**348**-368	**382-402**	405-**425**	442-**462**	471-491
TMpred	35-**56**	75-91	**100-119**	**125-150**	160-**177**	200-**218**	301-319	**348**-367	385-401	**408**-428	**437**-467	**472-490**
TMAP	29-52	72-94	99-**119**	129-149	159-179	193-217	**311**-334	344-**372**	379-**402**	406-430	**437**-457	467-487
MEMSTAT	37-60	76-**93**	**100-119**	126-142	**154-177**	**198**-217	304-323	**348**-366	**382**-399	**408**-431	439-**462**	**472-490**
TMHMM2	**34-56**	**71-93**	**100**-122	127-149	**154**-176	196-**218**	**311**-333	**348**-370	**382**-401	411-433	440-**462**	**472-490**

Figure 4 Topological model of TbNrt2

(**A**) Structural organization of the TbNrt2 polypeptide according to the consensus prediction of five prediction methods. Amino acid residues that are identical in the alignment of all available NRT2 fungal sequences are shaded grey; TM helices are labelled with Roman numerals. Amino acids corresponding to the MFS and NS motifs, and to the putative protein kinase C phosphorylation site (SPR) are enclosed in dark circles; the two arginine residues (located in TM helices II and VIII) that are positionally equivalent to those required for high-affinity nitrate transport by *A. nidulans* NrtA [39] are represented as white letters on a black background. (**B**) Helix boundaries predicted by concordant prediction programs. Boundaries chosen for the TbNrt2 topology model shown in (**A**) are in bold.

intracellular) orientation was predicted by HMMTOP. Following the 'majority-vote' criterion, which yielded reliable topologies when applied to membrane proteins of known structure analysed with different prediction methods [37], we considered as valid the 12 TM helices/$N_{IN}C_{IN}$ model shown in Figure 4(A). As shown in Figure 4(B), there was generally a good agreement between the five concordant programs not only on the general predicted topology, but also on the identification of putative TM regions. The five programs, however, produced slightly different results as to the precise localization of the borders of individual membrane-spanning helices. To identify the most likely borders of individual TM helices, we again relied on a majority-vote criterion, and incorporated into the model of Figure 4(A) consensus border residues suggested by at least three of the five prediction methods. For all those instances in which the above consensus criterion was not applicable, we resorted to SSpro8, a neural network program capable of predicting eight different types of secondary structures in globular proteins. This allowed us to identify individual positions at which α-helices are expected to be interrupted by β-turns, a diagnostic feature of TM helix-connecting loops in membrane proteins. In accordance with the general topology of NRT2 transporters [1], the N- and C-termini of TbNrt2 and its TM-helix-connecting loops are all quite short (4–34 amino acids, together corresponding to less than 30 % of the entire protein), except for the 93-amino-acid loop interposed between TM helices VI and VII. This large loop, along with a fairly short C-terminal tail, is a typical signature of fungal NRT2s [39]. It accounts for approx. 18 % of the entire protein by itself and was thus used as an antigen for anti-TbNrt2 antibody production (Figure 2A). Also apparent is the predomiance of positively charged amino acid residues associated with both extracellular and intracellular loops (Figure 4A), the main exception being the negative charge of the large VI–VII loop (a feature that suggests the existence of electrostatic interactions between oppositely charged cytoplasm-facing regions of TbNrt2). The reliability of this model was also supported by the presence, within such a loop (positions 233–235), of a putative protein kinase C phosphorylation site (Ser/Thr-Xaa-Arg/Lys, where Xaa is any amino acid) found previously in a topologically equivalent position in other NRT2 transporters [1]. Additional diagnostic sequencess were the two MFS (positions 90–99 and 364–372) and NS (nitrate signature; positions 150–171 and 437–454) motifs typically associated with NRT2 transporters, and two positionally conserved arginine residues (within TM helices II and VIII) that are required for high-affinity nitrate transport by *A. nidulans* NrtA [39].

By referring to the topological model described above, the TbNrt2 polypeptide was compared with homologous sequences from other fungi. Amino acid residues that were conserved in all NRT2 transporters (Figure 4A) were dislocated along the entire sequence. Conservation was maximal in TM helices I, IV and V (46–52 % identity), whereas it was nearly absent in loops VII–VIII, IX–X, XI–XII and in the region interposed between the end of helix XII and the C-terminus. As apparent in Figure 5, three separate groups, corresponding to unicellular ascomycetes, such as *Ha. polymorpha*, filamentous ascomycetes and basidiomycetes, are discernible in the NRT2 cluster. TbNrt2 belongs to the filamentous ascomycetes group, with NtrB from *A. nidulans* as its closest homologue.

TbNrt2 expression in mycelia cultured under different nitrogen nutritional regimens

RNase-protection and RNA gel-blot assays were conducted to determine *TbNrt2* mRNA levels in *T. borchii* mycelia subjected to different nitrogen status perturbations. We initially examined the response of *TbNrt2* to nitrogen deprivation. As shown in

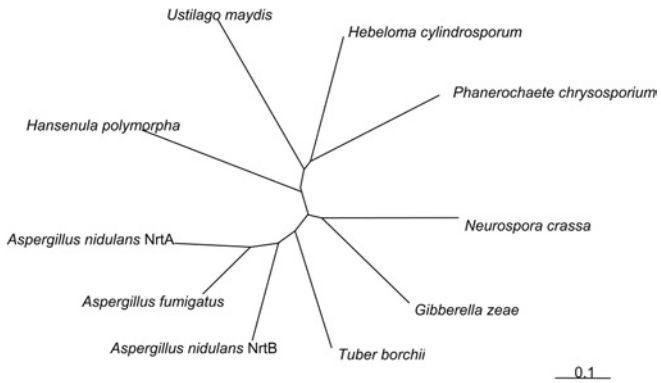

Figure 5 Phylogenetic relationships among fungal NRT2 transporters

A radial phylogenetic tree was constructed with neighbour-joining on the basis of the alignment of fungal NRT2 polypeptides homologous with TbNrt2; branches are drawn to scale (the scale bar corresponds to 0.1 changes per site). The NCBI accession numbers of the sequences used for tree construction are: CAB60009 (*He. cylindrosporum* Nrt2), P22152 (*A. nidulans* CrnA), AAL50818 (*A. nidulans* NrtB), CAD28427 (*A. fumigatus* CrnA), CAD71077 (*N. crassa* Nit-10), CAA11229 (*Ha. polymorpha* Ynt1), AF462038 (*T. borchii* TbNrt2), PC.9.52.1 (*Phanerochaete chrysosporium*; Joint Genome Institute), XP_401464 (*Ustilago maydis*), XP_380592 (*Gibberella zeae*).

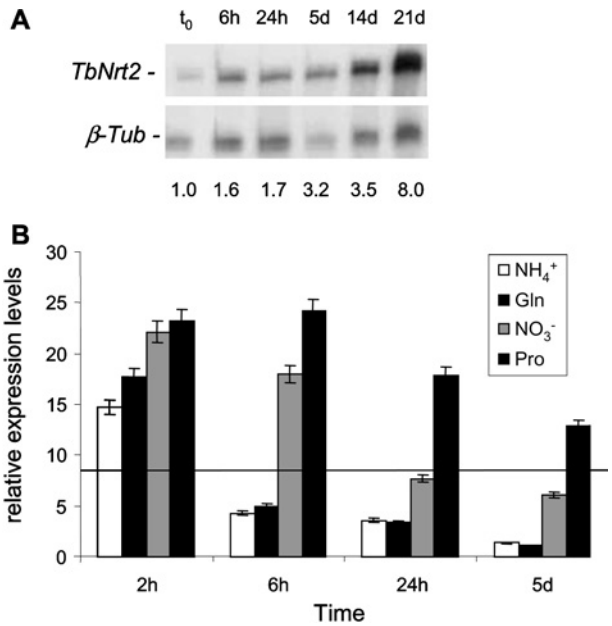

Figure 6 Nitrogen-status-dependent modulation of the *TbNrt2* mRNA

(**A**) Time course of *TbNrt2* up-regulation in nitrogen-starved *T. borchii* mycelia. *TbNrt2* mRNA levels were determined by RNase protection assays conducted on mycelia grown for 10 days on complete SSM (t_0) and then transferred for the indicated lengths of time to nitrogen-free SSM. A *T. borchii* β-tubulin (*β-Tub*) antisense riboprobe was included in all assays as an internal standard. The bands shown, which correspond to protection products of the *TbNrt2* and *β-Tub* riboprobes, were visualized by autoradiography and quantified by phosphorimaging. Relative transcript abundance values (reported below each lane) were calculated by dividing the volumes of the *TbNrt2* signals by the volumes of the corresponding *β-Tub* signals, followed by normalization with respect to *TbNrt2* abundance in unshifted (t_0) controls. (**B**) *TbNrt2* modulation following supplementation of nitrogen-starved mycelia with various nitrogen sources. Results obtained from RNase protection assays conducted on mycelia cultured for 21 days in nitrogen-free medium and then shifted for the indicated lengths of time to modified SSMs containing either NH_4Cl (NH_4^+), L-glutamine (Gln), KNO_3 (NO_3^-), or L-proline (Pro) (each at a 4 mM final concentration) as the sole nitrogen sources are shown. Data analyses and quantification were performed as in (**A**). Relative *TbNrt2* transcript levels, normalized with respect to nitrogen-sufficient 10-day-old mycelia, are reported on the *y*-axis; relative *TbNrt2* abundance in unshifted mycelia, nitrogen-deprived for 21 days, is indicated by the horizontal line.

Figure 6(A), *TbNrt2* mRNA was up-regulated as early as 6 h from transfer to nitrogen-free medium and increased further thereafter. Similar results were obtained using RNA gel-blot analysis (results not shown, but see Figure 7B).

The reverse response, i.e. *TbNrt2* down-regulation following resupplementation of various nitrogen sources, was investigated next. As shown in Figure 6(B), this was generally faster than nitrogen-starvation-induced up-regulation and was always preceded by a transient increase in *TbNrt2* mRNA levels. Ammonium and glutamine displayed the strongest down-regulating capacity. They reduced *TbNrt2* expression to levels lower than those of t_0 (time 0) controls (i.e. unshifted mycelia cultured for 21 days in nitrogen-free medium) in less than 6 h and turned it off almost completely in approx. 5 days. A much more persistent increase in *TbNrt2* abundance was observed with proline, a poor nitrogen source for *T. borchii* ([18,22], and below), which failed to lower *TbNrt2* expression below t_0 control levels, even after 5 days of supplementation. An intermediate response, with a marked increase in *TbNrt2* abundance up to 6 h, followed by a gradual decrease thereafter, was observed with nitrate. The transient up-regulation observed after ammonium or glutamine supplementation was as yet unexplained. The more substantial and long-lasting increase in *TbNrt2* levels observed with the other two nitrogen compounds may, however, reflect the extremely poor nitrogen source capacity of proline (and thus the unrelenting nitrogen deprivation status imposed by the supplementation of this amino acid) and nitrate-mediated induction of the NT mRNA as in other fungi [3,4,6,9]. We tested the latter hypothesis by measuring *TbNrt2* expression in nitrogen (ammonium)-sufficient mycelia transferred for various lengths of time to a medium containing 4 mM $NaNO_3$ (or $NaNO_2$) as the sole source of nitrogen. As shown in Figure 7(A), *TbNrt2* mRNA was indeed up-regulated (approx. 4-fold) as early as 24 h from exposure to nitrate and increased further (up to approx. 7-fold) within the 5-day observation window of this experiment. A smaller, but significant, up-regulation was also observed upon shift to an nitrite-containing medium, whereas no variation in *TbNrt2* expression was observed following transfer to the same ammonium-containing medium used for the initial growth of mycelia (results not shown, but see below). An RNA gel-blot experiment was then carried out to examine the effect of nitrate when supplied in combination with other nitrogen sources and to compare the outcome of nitrogen starvation and nitrate supplementation on both *TbNrt2* and on the adjacent *tbnr1* gene (see Figure 1B). As shown in Figure 7(B), *TbNrt2* expression was similarly up-regulated following transfer to either nitrogen-free or nitrate-supplemented medium, but not to ammonium- or glutamine-containing medium. Also apparent is the extremely poor N-source capacity of proline; in its presence, *TbNrt2* levels were as high as in N-starved mycelia (Figure 7B, lanes Pro, -N and NO_3^-) and it did not interfere with nitrate-induced *TbNrt2* up-regulation (Figure 7B, compare lane $+NO_3^-$/Pro with lanes $+NO_3^-/NH_4^+$ and $+NO_3^-$/Gln). Importantly, the data also show the distinct response profile of the *tbnr1* gene, which readily responded to nitrate supplementation but not to nitrogen deprivation.

As shown by the immunoblot in Figure 7(C), derepression of the *TbNrt2* mRNA following nitrogen deprivation and its induction by nitrate was accompanied by similar variations at the protein level. The main difference (reproducibly observed in three independent experiments) was that protein accumulation under both nitrogen-deprivation and nitrate-supplementation conditions was usually less persistent than transcript up-regulation.

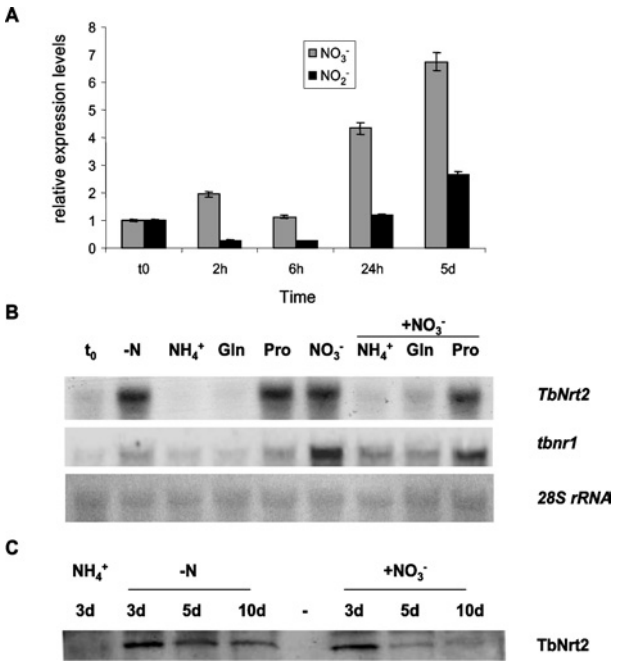

Figure 7 Nitrogen-source-dependent regulation of *TbNrt2* and *tbnr1*

(**A**) Results obtained from RNase protection assays conducted on mycelia cultured for 10 days in ammonium-containing SSM and then shifted for the indicated lengths of time to modified SSMs containing either KNO_3 or KNO_2 as the sole nitrogen sources. Data analyses and quantification were performed as in Figure 6(A). (**B**) RNA gel-blot analysis of mycelia cultured for 10 days in ammonium-containing SSM and then shifted for 5 days to SSM lacking any source of nitrogen (-N), to SSM containing either NH_4Cl (NH_4^+), glutamine (Gln), proline (Pro) or nitrate (NO_3^-) as the sole nitrogen sources, or to a modified SSM containing KNO_3 along with each of the indicated nitrogen compounds (NH_4^+, Gln or Pro); all nitrogen compounds were added at a final concentration of 4 mM. The same blot was separately hybridized with either a *TbNrt2* or a *tbnr1* probe as indicated. Methylene-Blue-stained 28 S rRNA bands, used as loading controls, are shown below each lane. (**C**) Immunoblot analysis of TbNrt2 protein levels in crude membrane preparations (20 μg of total protein for each sample) derived from mycelia cultured for 10 days in ammonium-containing SSM and then shifted for the indicated lengths of time to either the same medium (NH_4^+), to SSM lacking any source of nitrogen (-N) or to SSM supplemented with 4 mM KNO_3 ($+NO_3^-$); no immunopositive signal was detected upon hybridization with pre-immune serum.

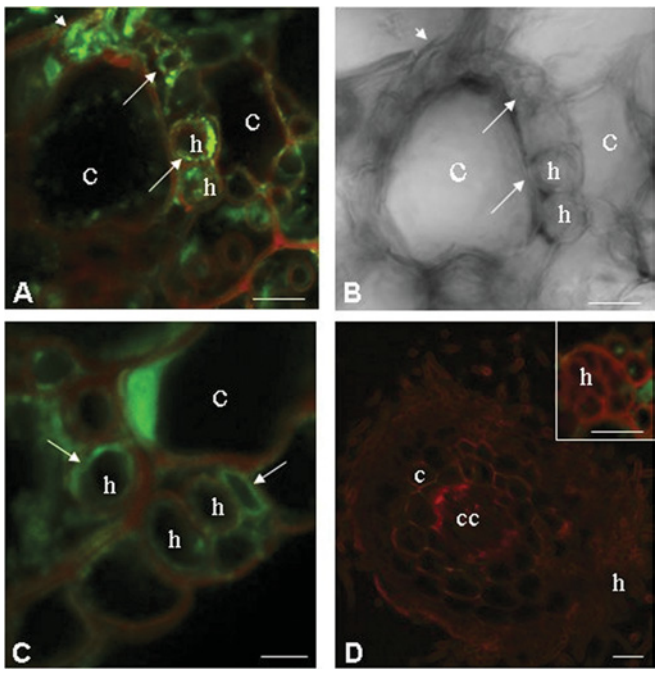

Figure 8 Immunofluorescence localization of TbNrt2 in ectomycorrhizae

(**A**) Immunodetection of TbNrt2 in Hartig net hyphae (h), close to root cortical cells (c), within sectioned tips from *T. borchii*/*C. incanus* mycorrhizae analysed by confocal microscopy. Arrows point to the green line labelling, associated with the fungal membrane, observed in transversally sectioned hyphae; arrowheads point to the fluorescent green signal detected in tangentially sectioned hyphae (bar = 10 μm). Under the confocal microscopy analysis conditions used to visualize the FITC-labelled secondary antibody, the fungal wall displayed a characteristic red autofluorescence. (**B**) Transmitted-light view of the same sample shown in (**A**); symbols and magnification are the same as in (**A**). (**C**) Immunodetection of TbNrt2 (arrows) associated with the fungal membrane of developing mantle hyphae (h) ensheathing root cortical cells (c); visualization conditions and magnification are the same as in (**A**). (**D**) Low-magnification image (bar = 25 μm) of a control section visualized by confocal microscopy in the absence of the primary antibody. The red autofluorescence is associated with plant and fungal cell walls; cc indicates the central cylinder, the other symbols are as specified in (**A**). A higher magnification image (bar = 13 μm) of a different section, visualized by confocal microscopy using the pre-immune serum in place of anti-TbNrt2 antibody, is shown in the inset; no specific signal was detected in Hartig net or in mantle-forming hyphae (h).

TbNrt2 localization in mycorrhizae

Anti-TbNrt2 antibodies were used to examine the expression of the TbNrt2 transporter and its localization in *T. borchii*/*C. incanus* ectomycorrhizae [29]. A fairly strong and specific TbNrt2-associated signal was detected by immunofluorescence, which also revealed a differential labelling of the hyphae depending on their location. Labelling was more pronounced in Hartig-net- and mantle-forming (Figures 8A and 8C respectively) hyphae that were in close contact with the roots than in extraradical hyphae. The green fluorescent signal was predominantly associated with the inner part of the fungal wall, whose scaffold was revealed by a red autofluorescence. This green line signal, which was easily appreciated in transversally sectioned hyphae, can be attributed to the fungal membrane (Figures 8A and 8C). By contrast, a more extensive, but blurred, signal was observed in tangentially sectioned hyphae (Figure 8A). No specific signal was detected when the primary antibody was omitted (Figure 8D) or the pre-immune serum was used in place of anti-TbNrt2 antibody (Figure 8D, inset). Some labelling was occasionally observed in the cytoplasm of plant cells with both the the anti-TbNrt2 antibody and the pre-immune serum. This labelling, however, always appeared as an intense intracellular green spot which was easily distinguishable from the fungus-associated signal, suggesting non-specific binding to, and detection of, some unrelated plant antigen.

DISCUSSION

The TbNrt2 transporter

The predicted topology and secondary structure of TbNrt2 resemble those of NRT2 transporters from non-mycorrhizal fungi characterized previously. The most prominent among these shared features is the large VI–VII loop we used as antigen for antibody production, the MFS and NS motifs, and two positionally conserved arginine residues that are required for high-affinity transport by *A. nidulans* NrtA [39]. Some less common features were revealed by functional complementation assays in *Ha. polymorpha*, which also highlighted the potentialities of this yeast as a model system for the study of heterologous NTs. These include the ability of TbNrt2 to support high-affinity transport of nitrate and nitrite, but not chlorate ions. With the sole exception of *A. nidulans* NrtA assayed in *Xenopus* oocytes [5], the nitrite transport capacity of other fungal NTs has not, so far, been determined directly. However, the observation that growth on nitrite is not impaired in either an *A. nidulans nrtA*/*ntrB* double mutant [6], or in an *N. crassa nit-10* mutant [9], has been taken

as an indication that none of the above NTs is capable of nitrite transport. TbNrt2 is distinct from both *Neurospora* Nit-10 and *Aspergillus* NrtA, but not NrtB, also with regard to chlorate (and contaminating chlorite) tolerance. The lack of any influence on chlorate sensitivity, compared with the corresponding NT-disrupted strain, is a common property of Ynt1 and TbNrt2, and of its closest relative, NtrB (Figure 5). An amino acid residue potentially involved in chlorate tolerance is Arg^{188}, located in the outer loop interposed between TM helices V and VI (Figure 4A), which is conserved positionally in TbNrt2, Ynt1 and NtrB, but not in NtrA. The cellular and molecular tools described in the present study, coupled with site-directed mutagenesis, will allow testing of this hypothesis. Chlorate tolerance, resulting from the inability to internalize this toxic ion, may be especially relevant if one considers that: (i) chlorate is a soil pollutant which is also used as a non-specific herbicide; (ii) there is an intimate association (and metabolite exchange) between mycorrhizal fungi and their host plants; and (iii) TbNrt2 is expressed in mycorrhizae, where it preferentially accumulates in symbiotic hyphae that are in close contact with the roots (Figure 8). Interestingly, a similar trait, namely resistance to phosphinotricin {the active ingredient of the herbicide glufosinate (4-[hydroxy(methyl)phosphinoyl]-DL-homoalanine)}, has been documented previously for *T. borchii* glutamine synthetase [22].

Mode of regulation of TbNrt2

More distinguishing was the mode of regulation of TbNrt2, which was found to be induced by nitrate, as in most nitrate-using organisms [1–3,10], but also up-regulated through a nitrate independent derepression mechanism triggered by nitrogen starvation. An exception to this nitrogen-deprivation-based control was the transient *TbNrt2* up-regulation observed after ammonium or glutamine refeeding of extensively starved mycelia (Figure 6B). In keeping with the almost complete depletion of the amino acid pool revealed by GLC/MS analysis of mycelia grown for more than 5 days on nitrogen-free medium (results not shown), this may reflect rapid nitrogen assimilation and transient *TbNrt2* synthesis due to delayed accumulation of repressive nitrogen compounds in severely starved cells. What is also intriguing is the co-existence (and apparent redundancy) of nitrate-dependent induction in a system that is primarily controlled by nitrogen-source depletion. TbNrt2 levels were nearly the same under both conditions ($-$N and $+NO_3^-$; Figure 7B), but TbNrt2 up-regulation in response to nitrate supplementation was generally faster than that brought about by nitrogen depletion (Figures 6A and 7A), and even more so when nitrate was supplied to mycelia starved previously (Figure 6B). Thus a possible advantage of this dual mode of regulation may be a faster up-regulation of nitrate transport when both conditions are met.

Although as yet uncharacterized from a functional point of view, an NT displaying the same kind of nitrate-independent up-regulation as *TbNrt2* has been described recently in the mycorrhizal basidiomycete *He. cylindrosporum* [23]. Interestingly, the occurrence of a similar mode of regulation has been inferred previously from physiological data obtained in nitrophilic yeasts such as *Sporobolomyces roseus*, *Candida nitratophila* and *Rhodotorula glutinis* [40,41] and in the mycorrhizal basidiomycete *Rhizopogon roseolus* [11]. The above fungi colonize different environments and are not closely related evolutionarily to each other, nor to *T. borchii*. Therefore nitrate-independent up-regulation of nitrate transport does not represent a conserved feature shared by a restricted group of phylogenetically related species, nor does it seem to be related to a particular growth environment. Instead, it appears to be a fairly ancient regulatory strategy that predated the appearance of multicellular fungi and is now found in filamentous symbiotic ascomycetes and basidiomycetes.

Nitrate-independent TbNrt2 up-regulation and the symbiotic lifestyle

What may then be the functional implications of nitrate-independent up-regulation and the reason(s) for its selective occurrence in mycorrhizal fungi? The most obvious answer is that this regulatory strategy is somehow related to the ability of these organisms to sustain host-plant nitrogen nutrition even under conditions in which the concentration of available nitrate may not be sufficient to induce nitrate assimilation genes. Under these conditions, nitrate-independent up-regulation would also solve the problem of nitrate uptake under 'pre-induction' conditions (i.e. the entrance of the very first nitrate ions that are taken up before fully executed nitrate-dependent induction). This strategy would enable the fungus, and its host plant, to cope with the low and fluctuating (by more than four orders of magnitude) nitrate concentrations found in most natural, especially forest, soils. In addition, simultaneous up-regulation of nitrate and ammonium transporters by the same nitrogen shortage stimulus [18,21,22] may allow a more balanced nitrogen nutrition when both inorganic nitrogen sources are available in limited amounts. Although the estimated K_m of TbNrt2 for nitrate (4.7 μM) is in the lower range of the values reported so far for fungal NTs, the obvious disadvantage of this mode of regulation would be the high biosynthetic cost of nitrate assimilation component expression (NT, NR and NIR) in the presence of exceedingly low nitrate concentrations, far below such K_m. Noteworthy, in this regard, is the observation that the NR gene of *T. borchii* (*tbnr1*), at variance with *TbNrt2* and with the corresponding genes of *He. cylindrosporum* (*nrt2* and *nar1*; [16,23]), is expressed at basal levels under nitrogen-deprivation conditions and requires nitrate-mediated induction as in most organisms. Basal *tbnr1* expression in nitrogen-deficient mycelia (revealed by the faint hybridization signal in Figure 7B) would alleviate the biosynthetic cost of NR overexpression in the presence of low (non-inducing) nitrate concentrations. Under the same conditions, however, it would provide enough enzyme for nitrate reduction, which has been shown to be functionally coupled with nitrate uptake [42].

Regulatory variation is one of the main pathways for organism evolution and specialization. It is tempting to speculate that the regulatory diversity of nitrate assimilation genes highlighted in the present study may be one of the factors that determine the environmental adaptation capacity of mycorrhizal (and non-mycorrhizal) fungi. Experimental verification of this hypothesis, as well as more detailed studies of nitrogen-metabolism regulation under symbiotic conditions, will be facilitated by the recent development of a genetic transformation system for *T. borchii* [43].

We thank Dr Angelo Viotti (Istituto di Biologia e Biotecnologia Agraria, CNR, Milano, Italy) for the gift of the *T. borchii* cDNA library. The help of Elisabetta Soragni and Daniela Pecorari in an early stage of this study is also gratefully acknowledged. The present study was supported by grants from the Consiglio Nazionale delle Ricerche, the Regione Emilia-Romagna and the University of Parma (FIL2004) to S.O., from the Fondo per gli Investimenti della Ricerca di Base ('Genomica funzionale dell'interazione tra piante e microrganismi') to A.B. and P.B., and by grant BFU2004-01012 from Ministerio de Educación y Ciencia, Spain, to J.M.S. Y.M. is a Fellow of the Ministerio de Educación y Ciencia, Spain.

REFERENCES

1 Forde, B. G. (2000) Nitrate transporters in plants: structure, function and regulation. Biochim. Biophys. Acta **1465**, 219–235

2 Glass, A. D., Britto, D. T., Kaiser, B. N., Kinghorn, J. R., Kronzucker, H. J., Kumar, A., Okamoto, M., Rawat, S., Siddiqi, M. Y., Unkles, S. E. and Vidmar, J. J. (2002) The regulation of nitrate and ammonium transport systems in plants. J. Exp. Bot. **53**, 855–864

3 Siverio, J. M. (2002) Assimilation of nitrate by yeasts. FEMS Microbiol. Rev. **26**, 277–284

4 Unkles, S. E., Hawker, K. L., Grieve, C., Campbell, E. I., Montague, P. and Kinghorn, J. R. (1991) *crnA* encodes a nitrate transporter in *Aspergillus nidulans*. Proc. Natl. Acad. Sci. U.S.A. **88**, 204–208

5 Zhou, J. J., Trueman, L. J., Boorer, K. J., Theodoulou, F. L., Forde, B. G. and Miller, A. J. (2000) A high affinity fungal nitrate carrier with two transport mechanisms. J. Biol. Chem. **275**, 39894–39899

6 Unkles, S. E., Zhou, D., Siddiqi, M. Y., Kinghorn, J. R. and Glass, A. D. (2001) Apparent genetic redundancy facilitates ecological plasticity for nitrate transport. EMBO J. **20**, 6246–6255

7 Perez, M. D., Gonzalez, C., Avila, J., Brito, N. and Siverio, J. M. (1997) The *YNT1* gene encoding the nitrate transporter in the yeast *Hansenula polymorpha* is clustered with genes *YNI1* and *YNR1* encoding nitrite reductase and nitrate reductase, and its disruption causes inability to grow in nitrate. Biochem. J. **321**, 397–403

8 Machin, F., Medina, B., Navarro, F. J., Perez, M. D., Veenhuis, M., Tejera, P., Lorenzo, H., Lancha, A. and Siverio, J. M. (2004) The role of Ynt1 in nitrate and nitrite transport in the yeast *Hansenula polymorpha*. Yeast **21**, 265–276

9 Gao-Rubinelli, F. and Marzluf, G. A. (2004) Identification and characterization of a nitrate transporter gene in *Neurospora crassa*. Biochem. Genet. **42**, 21–34

10 Marzluf, G. A. (1997) Genetic regulation of nitrogen metabolism in the fungi. Microbiol. Mol. Biol. Rev. **61**, 17–32

11 Gobert, A. and Plassard, C. (2002) Differential NO_3^- dependent patterns of NO_3^- uptake in *Pinus pinaster*, *Rhizopogon roseolus* and their ectomycorrhizal association. New Phytol. **154**, 509–516

12 Read, D. J. and Perez-Moreno, J. (2003) Mycorrhizas and nutrient cycling in ecosystems: a journey towards relevance? New Phytol. **157**, 475–492

13 Soragni, E., Bolchi, A., Balestrini, R., Gambaretto, C., Percudani, R., Bonfante, P. and Ottonello, S. (2001) A nutrient-regulated, dual localization phospholipase A_2 in the symbiotic fungus *Tuber borchii*. EMBO J. **20**, 5079–5090

14 Javelle, A., André, B., Marini, A. M. and Chalot, M. (2003) High-affinity ammonium transporters and nitrogen sensing in mycorrhizas. Trends Microbiol. **11**, 53–55

15 Javelle, A., Chalot, M., Brun, A. and Botton, B. (2004) Nitrogen transport and metabolism in mycorrhizal fungi and mycorrhizas. In Plant Surface Microbiology (Varma, A., Abbott, L., Werner, D. and Hampp, R., eds.), pp. 394–429, Springer-Verlag, Berlin-Heidelberg

16 Jargeat, P., Gay, G., Debaud, J. C. and Marmeisse, R. (2000) Transcription of a nitrate reductase gene isolated from the symbiotic basidiomycete fungus *Hebeloma cylindrosporum* does not require induction by nitrate. Mol. Gen. Genet. **263**, 948–956

17 Javelle, A., Rodriguez-Pastrana, B. R., Jacob, C., Botton, B., Brun, A., André, B., Marini, A. M. and Chalot, M. (2001) Molecular characterization of two ammonium transporters from the ectomycorrhizal fungus *Hebeloma cylindrosporum*. FEBS Lett. **505**, 393–398

18 Montanini, B., Moretto, N., Soragni, E., Percudani, R. and Ottonello, S. (2002) A high-affinity ammonium transporter from the mycorrhizal ascomycete *Tuber borchii*. Fungal Genet. Biol. **36**, 22–34

19 Vallorani, L., Polidori, E., Sacconi, C., Agostini, D., Pierleoni, R., Piccoli, G., Zeppa, S. and Stocchi, V. (2002) Biochemical and molecular characterization of NADP glutamate dehydrogenase from the ectomycorrhizal fungus *Tuber borchii*. New Phytol. **154**, 779–790

20 Guescini, M., Pierleoni, R., Palma, F., Zeppa, S., Vallorani, L., Potenza, L., Sacconi, C., Giomaro, G. and Stocchi, V. (2003) Characterization of the *Tuber borchii* nitrate reductase gene and its role in ectomycorrhizae. Mol. Genet. Genomics **269**, 807–816

21 Javelle, A., Morel, M., Rodriguez-Pastrana, B. R., Botton, B., André, B., Marini, A. M., Brun, A. and Chalot, M. (2003) Molecular characterization, function and regulation of ammonium transporters (Amt) and ammonium-metabolizing enzymes (GS, NADP-GDH) in the ectomycorrhizal fungus *Hebeloma cylindrosporum*. Mol. Microbiol. **47**, 411–430

22 Montanini, B., Betti, M., Marquez, A. J., Balestrini, R., Bonfante, P. and Ottonello, S. (2003) Distinctive properties and expression profiles of glutamine synthetase from a plant symbiotic fungus. Biochem. J. **373**, 357–368

23 Jargeat, P., Rekangalt, D., Verner, M. C., Gay, G., Debaud, J. C., Marmeisse, R. and Fraissinet-Tachet, L. (2003) Characterisation and expression analysis of a nitrate transporter and nitrite reductase genes, two members of a gene cluster for nitrate assimilation from the symbiotic basidiomycete *Hebeloma cylindrosporum*. Curr. Genet. **43**, 199–205

24 Sambrook, J. and Russell, D. W. (2001) In Molecular Cloning: A Laboratory Manual, Cold Spring Harbor Laboratory Press, Cold Spring Harbor, N.Y.

25 Perdomo, G., Navarro, F. J., Medina, B., Machin, F., Tejera, P. and Siverio, J. M. (2002) Tobacco *Nia2* cDNA functionally complements a *Hansenula polymorpha* yeast mutant lacking nitrate reductase: a new expression system for the study of plant proteins involved in nitrate assimilation. Plant Mol. Biol. **50**, 405–413

26 Faber, K. N., Haima, P., Harder, W., Veenhuis, M. and Ab, G. (1994) Highly-efficient electrotransformation of the yeast *Hansenula polymorpha*. Curr. Genet. **25**, 305–310

27 Thompson, J. D., Higgins, D. G. and Gibson, T. J. (1994) CLUSTAL W: improving the sensitivity of progressive multiple sequence alignment through sequence weighting, position-specific gap penalties and weight matrix choice. Nucleic Acids Res. **22**, 4673–4680

27a Thompson, J. D., Gibson, T. J., Plewniak, F., Jeanmougin, F. and Higgins, D. G. (1997) The ClustalX windows interface: flexible strategies for multiple sequence alignment aided by quality analysis tools. Nucleic Acids Res. **25**, 4876–4882

28 Page, R. D. (1996) TreeView: an application to display phylogenetic trees on personal computers. Comput. Appl. Biosci. **12**, 357–358

29 Miozzi, L., Balestrini, R., Bolchi, A., Novero, M., Ottonello, S. and Bonfante, P. (2005) Phospholipase A_2 up-regulation during mycorrhiza formation in *Tuber borchii*. New Phytol. **167**, 229–238

30 Edelmann, S. E. and Staben, C. (1994) A statistical analysis of sequence features within genes from *Neurospora crassa*. Exp. Mycol. **18**, 70–81

31 Jones, D. T., Taylor, W. R. and Thornton, J. M. (1994) A model recognition approach to the prediction of all-helical membrane protein structure and topology. Biochemistry **33**, 3038–3049

32 Hofmann, K. and Stoffel, W. (1993) TMbase: a database of membrane spanning proteins segments. Biol. Chem. Hoppe-Seyler **374**, 166

33 Persson, B. and Argos, P. (1994) Prediction of transmembrane segments in proteins utilising multiple sequence alignments. J. Mol. Biol. **237**, 182–192

34 Claros, M. G. and von Heijne, G. (1994) TopPred II: an improved software for membrane protein structure predictions. Comput. Appl. Biosci. **10**, 685–686

35 Sonnhammer, E. L., von Heijne, G. and Krogh, A. (1998) A hidden Markov model for predicting transmembrane helices in protein sequences. Proc. Int. Conf. Intell. Syst. Mol. Biol. **6**, 175–182

36 Tusnady, G. E. and Simon, I. (1998) Principles governing amino acid composition of integral membrane proteins: application to topology prediction. J. Mol. Biol. **283**, 489–506

37 Nilsson, J., Persson, B. and von Heijne, G. (2000) Consensus predictions of membrane protein topology. FEBS Lett. **486**, 267–269

38 Baldi, P., Brunak, S., Frasconi, P., Soda, G. and Pollastri, G. (1999) Exploiting the past and the future in protein secondary structure prediction. Bioinformatics **15**, 937–946

39 Unkles, S. E., Rouch, D. A., Wang, Y., Siddiqi, M. Y., Glass, A. D. and Kinghorn, J. R. (2004) Two perfectly conserved arginine residues are required for substrate binding in a high-affinity nitrate transporter. Proc. Natl. Acad. Sci. U.S.A. **101**, 17549–17554

40 Ali, A. H. and Hipkin, C. R. (1985) Nitrate assimilation in the basidiomycete yeast *Sporobolomyces roseus*. J. Gen. Microbiol. **131**, 1867–1874

41 Ali, A. H. and Hipkin, C. R. (1986) Nitrate assimilation in *Candida nitratophila* and other yeasts. Arch. Microbiol. **144**, 263–267

42 Unkles, S. E., Wang, R., Wang, Y., Glass, A. D., Crawford, N. M. and Kinghorn, J. R. (2004) Nitrate reductase activity is required for nitrate uptake into fungal but not plant cells. J. Biol. Chem. **279**, 28182–28186

43 Grimaldi, B., de Raaf, M. A., Filetici, P., Ottonello, S. and Ballario, P. (2005) *Agrobacterium*-mediated gene transfer and enhanced green fluorescent protein visualization in the mycorrhizal ascomycete *Tuber borchii*: a first step towards truffle genetics. Curr. Genet. **48**, 69–74

Received 25 July 2005/12 September 2005; accepted 5 October 2005
Published as BJ Immediate Publication 5 October 2005, doi:10.1042/BJ20051199